VIP Graphene Nanoribbons Very Important Paper

International Edition: DOI: 10.1002/anie.201611834
German Edition: DOI: 10.1002/ange.201611834

Helically Coiled Graphene Nanoribbons

*Maxime Daigle, Dandan Miao, Andrea Lucotti, Matteo Tommasini, and Jean-François Morin**

Abstract: *Graphene is a zero-gap, semiconducting 2D material that exhibits outstanding charge-transport properties. One way to open a band gap and make graphene useful as a semiconducting material is to confine the electron delocalization in one dimension through the preparation of graphene nanoribbons (GNR). Although several methods have been reported so far, solution-phase, bottom-up synthesis is the most promising in terms of structural precision and large-scale production. Herein, we report the synthesis of a well-defined, helically coiled GNR from a polychlorinated poly(m-phenylene) through a regioselective photochemical cyclodehydrochlorination (CDHC) reaction. The structure of the helical GNR was confirmed by ^{1}H NMR, FT-IR, XPS, TEM, and Raman spectroscopy. This Riemann surface-like GNR has a band gap of 2.15 eV and is highly emissive in the visible region, both in solution and the solid state.*

Graphene can arguably be considered as one of the most interesting and versatile materials for practical applications as it exhibits outstanding charge transport properties, very high specific surface area, high thermal conductivity, and unrivaled mechanical strength.[1] In the form of a single-layer two-dimensional sheet however, graphene is a zero band gap semiconductor, or semimetal, which limits its use as an active component in traditional electronic devices.[2] To open the band gap, different strategies of quantum confinement have been developed.[3] In terms of atomic precision, the formation of graphene nanoribbons (GNRs) that restrict electron delocalization to one dimension is probably the most promising.[4] In fact, the band gap of GNRs can be precisely tuned by varying the width and edge configuration, providing GNRs with a wide range of optoelectronic properties.[5]

A promising approach to well-defined GNRs was pioneered by the Müllen group and consists of using standard solution-phase multistep synthesis.[6] The key step of their strategy is to submit a carefully designed polyphenylene precursor to a cyclodehydrogenation reaction (Scholl reaction) to obtain soluble and dispersible GNRs of different widths and edge configurations. Unlike other approaches, this bottom-up strategy allows for the synthesis of gram quantities of GNRs with control over edge structure and precise heteroatom doping.[7] Nevertheless, the Scholl reaction presents drawbacks that limit its usefulness for the synthesis of more complex GNRs architectures.[8] One of the most detrimental features is poor regioselectivity that can lead to structural defects that affect the properties of the GNRs.[9]

Recently, we reported the regioselective, solution-phase synthesis of nanographenes and GNR fragments using the photochemical cyclodehydrochlorination (CDHC) reaction on chlorine-containing polyphenylene precursors.[10] Since CDHC takes place in metal-free, milder reaction conditions than the Scholl reaction, it proceeds selectively and without the formation of side-products. Moreover, the CDHC reaction is compatible with different heterocycles and provides better control over the edge configuration of nanographenes than the Scholl reaction.

Herein, we successfully employ the CDHC reaction for the regioselective synthesis of the first polyhelicene-like GNR (helical graphene nanoribbon (HGNR); Figure 1). With

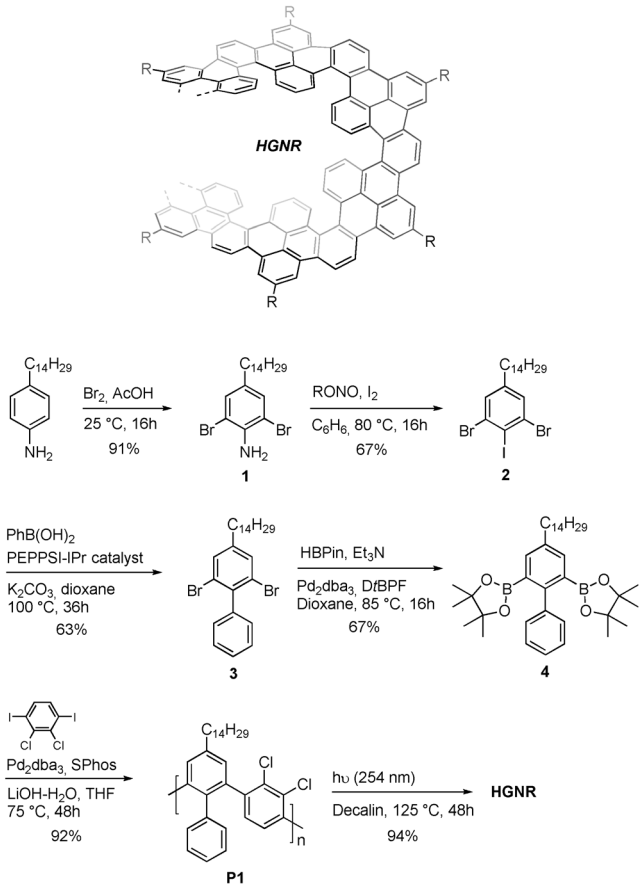

Figure 1. Synthesis of the helical graphene nanoribbon (HGNR), see text for details.

[*] M. Daigle, D. Miao, Prof. J.-F. Morin
Département de chimie and Centre de Recherche sur les Matériaux Avancés (CERMA)
Université Laval
1045 Ave de la Médecine, Québec, G1V 0A6 (Canada)
E-mail: jean-francois.morin@chm.ulaval.ca
A. Lucotti, M. Tommasini
Dipartimento di Chimica, Materiali e Ingegneria Chimica "G. Natta"
Politecnico di Milano
Piazza Leonardo da Vinci, 32, 20133 Milano (Italy)

Supporting information for this article can be found under: http://dx.doi.org/10.1002/anie.201611834.

 © 2017 Wiley-VCH Verlag GmbH & Co. KGaA, Weinheim

appropriate placement of chlorine atoms on a poly(*m*-phenylene) precursor, it is possible to force the formation of a conjugated helical structure resembling that of helicenes. This structure can be seen as the first example of a synthetic graphenic Riemann surface. Theoretical calculations suggest that such material could have outstanding inductor performance and thus be used as nanosolenoid.[11] The HGNR structure is characterized with a variety of techniques, including ^{1}H NMR, FTIR, XPS, TEM and Raman spectroscopy.

The syntheses of HGNR and its polymeric precursor P1 are shown in Figure 1. Starting from 4-tetradecylaniline, bromination at the 2 and 6 positions was performed using bromine, a subsequent one-pot diazotization/iodination reaction yielded compound **2**.[12] Then, a selective Suzuki–Miyaura coupling using PEPPSI-*i*Pr as the catalyst provides compound **3**,[13] which was subjected to a double borylation reaction in optimized conditions[14] to give monomer **4** in moderate yield. Finally, a Suzuki–Miyaura polymerization with 2,3-dichloro-1,4-diiodobenzene using $Pd_2dba_3{\cdot}CHCl_3$ as the catalyst and SPhos as the ligand provided P1 in 92% yield. This particular catalyst/ligand system proved to be efficient for the synthesis of poly(*m*-phenylene)s with few defects.[15]

For the synthesis of HGNR, P1 was dissolved in degassed decalin to a concentration of 0.002 M and the solution was irradiated using low-pressure mercury lamps ($\lambda_{em} = 254$ nm, 16×7.2 W) for 48 h under argon flow. Based on our previous study, this reaction time is sufficient to allow completion of the CDHC reaction.[10] It is worth mentioning that Mallory-type reactions that would lead to a planarization of the fjord region on the inner edge of the HGNR did not occur under these conditions since no oxidant was used.[10] Fortunately, photocyclization occurred as the solution went from colorless, blue fluorescent to orange, green–yellow fluorescent, which is indicative of significant structural changes in the π-conjugated backbone. After usual polymer treatment (see Supporting Information), an orange solid was obtained. Although HGNR exhibits relatively good solubility in organic solvents, complete drying makes it difficult to dissolve again, probably due to strong intermolecular interactions.

Size-exclusion chromatography (SEC) analysis was performed on P1 and HGNR using polystyrene standards and $CHCl_3$ as the eluent. P1 exhibits a unimodal molecular weight distribution with a M_n value of 16000 g mol^{-1}, corresponding to a degree of polymerization (DP) of 32 units, and a polydispersity index (PDI) of 2.0 (see Figure S11). As expected, HGNR exhibits a slightly lower M_n value (15200 g mol^{-1}, PDI = 1.9) than P1 due to the loss of HCl molecules and the formation of a compact helical π-conjugated structure with a lower hydrodynamic radius compared to the linear precursor P1. The decrease of the M_n value upon covalent immobilization of a helical structure has been reported previously for poly(*m*-phenyleneethynylene) foldamers.[16] Considering that one helical pitch consists of six monomeric units, a DP value of 32 represents approximately 5 helical pitches in average. The decrease in the M_n value also suggests that no intermolecular cross-linking reaction occurs upon irradiation of P1.

The ^{1}H NMR analysis of P1 and HGNR in $CDCl_3$ were conducted and the results are shown in Figure 2. As expected,

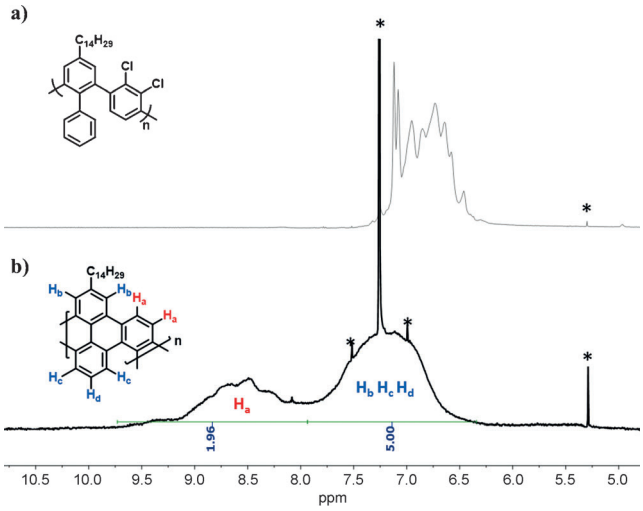

Figure 2. ^{1}H NMR spectrum of a) P1 in $CDCl_3$ at 25 °C and b) HGNR in $CDCl_3$ at 60 °C. Peaks marked with an asterisk are attributed to residual solvent.

the spectrum of P1 exhibits rather broadened signals compared to its monomeric analogues. The ensemble of aromatic protons produce an unresolved broad peak centered at $\delta =$ 6.8 ppm. After irradiation to produce HGNR, the spectrum flattens, especially in the aromatic region, and the peaks are shifted downfield as a result of the formation of a rigid structure. The presence of very broad peaks in the aromatic region can also be attributed to the coexistence of different conformations with different symmetries owing to the presence of a contorted region (fjord region) on the inner edge of the HGNR. This line broadening behavior was observed and studied in case of [10]cloverphene[17] and other hexabenzotriphenylene motifs.[18] As shown in Figure 2b, a very broad signal centered at $\delta = 8.6$ appears, and the broad signal of P1 originally centered at $\delta = 6.8$ ppm shifts downfield to 7.2 ppm. The resonance at $\delta = 8.6$ ppm can be ascribed to the outer edge protons H_a of the so-called bay region, whereas that at 7.3 ppm is attributed to the outer protons H_b and inner protons H_c and H_d. Many attempts to obtain a MALDI-TOF MS spectrum of HGNR failed to produce meaningful results. Thus, X-ray photoelectron spectroscopy (XPS) analysis was performed to assess the disappearance of the chlorine atoms and the formation of a graphenic structure after irradiation. As expected, P1 exhibits a peak at 202 eV, corresponding to the Cl2p band (Figure S19). Interestingly, the XPS spectrum of HGNR shows no trace of this peak, meaning that the CDHC reaction is complete and that no chlorine-containing side-product has been formed during the reaction (Figure S20).

Figure 3 shows the FTIR spectra of P1 and HGNR. The success of the CDHC reaction can be assessed with the band at 4054 cm^{-1}, which is associated with the free rotation of the phenyl group.[19] While this band can clearly be seen in the spectrum of P1, it is essentially absent in that of HGNR,

 © 2017 Wiley-VCH Verlag GmbH & Co. KGaA, Weinheim

These are not the final page numbers!

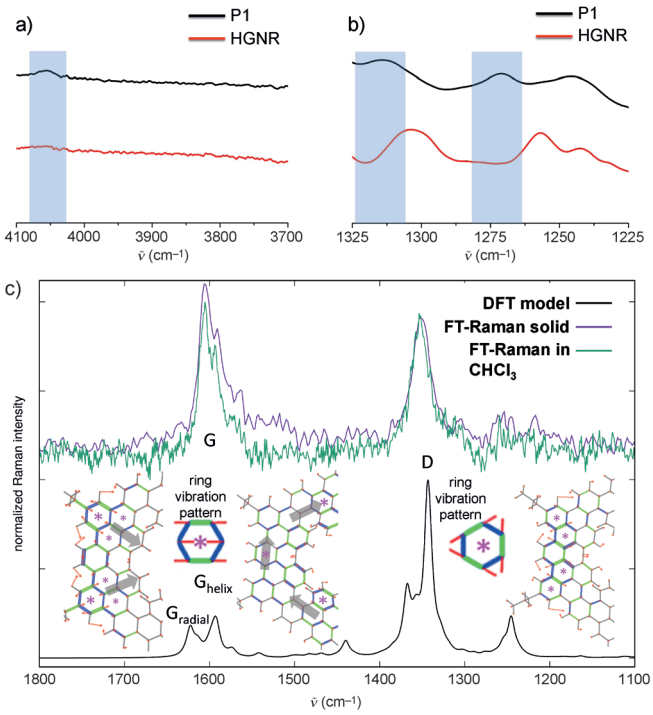

Figure 3. a),b) FTIR spectrum of P1 (black lines) and HGNR (red lines) Blue bars highlight spectral differences, see text for details. c) FT-Raman spectrum of HGNR in the solid state and $CHCl_3$ solution (10 mg mL^{-1}). Nuclear displacement patterns are also shown for characteristic G and D modes (see text for clarification. Just a section of the helical model is displayed): red arrows represent displacement vectors; CC bonds are represented as green and blue lines of different thicknesses according to their relative stretching (shrinking). The gray shaded arrows in the G_{helix} represent the direction of ring stretching along the helical structure. Selected rings are marked by asterisks to assist the reader in recognizing the characteristic ring vibration patterns associated to G and D modes (see Ref. [21] and Supporting Information for details).

indicating that the CDHC reaction went to near completion, as indicated by ^{1}H NMR spectroscopy. Moreover, the intensity of the bands at 3085, 3059, and 3027 cm^{-1} (see Figure S16), attributed to C–H aromatic stretching modes, decreases as fewer aromatic C–H groups are present in HGNR (Figure S16). The intensity of the bands associated with C–H stretching of alkyl chains remains constant (2920 and 2851 cm^{-1}) upon irradiation, indicating the integrity of the alkyl substituent (see Figure S17). Furthermore, bands associated with C=C stretching of chlorinated aromatic molecules at 1270 cm^{-1} and 1312 cm^{-1} completely vanish after irradiation (see Figure 3b). This observation, along with the decrease in intensity of bands that are associated with aromatic C–H out-of-plane located at 912 and 698 cm^{-1}, strongly suggest the loss of chlorine atoms and formation of HGNR (see Figure S18). The remaining C–H bonds of the aromatic backbone of the HGNR are responsible for the residual signal.

Raman spectroscopy of HGNR was carried out both in solution and the solid state to reveal the expected characteristic G and D peaks typical of nanostructured graphenes and nanoribbons. The solution and solid-state spectra are very similar, in agreement with UV/Vis data (see below). The experimental data of Figure 3c show structured G and D lines. Our DFT model of the Raman response allows assigning the main two G lines to collective ring stretching vibrations that occur either along the helix pattern (G_{helix}) or radially (G_{radial}). The helical coil of the ribbon induces this split of the G line, at difference from planar GNRs, which display a single G line.[20a,b,g,h] Similar to recently investigated GNRs, graphene molecules and helicenes,[20] the strongest feature in the D region is assigned to the expected vibrational pattern found in graphene structures.[21] The D and G modes of HGNR imply collective ring vibrations (marked by asterisks in Figure 3c) forming typical patterns, which closely match those theoretically predicted for graphene (see also Supporting Information).

Optical properties of HGNR were determined by UV/Vis and fluorescence spectroscopy and the results are shown in Figure 4. The UV/Vis spectrum of HGNR (Figure 4a) reveals absorption between 400 and 575 nm, with three vibronic bands at 409, 435, and 455 nm, indicating that a rigid, well-defined π-conjugated structure was formed upon irradiation. In contrast, the UV/Vis spectrum of P1 showed a featureless absorption band centered below 300 nm, which is indicative of a non-rigid, less conjugated structure. The solid-state absorption spectrum of HGNR exhibits a band that is slightly red-shifted (7 nm) compared to HGNR in solution. The small red shift in the λ_{max} value suggests that HGNR possesses

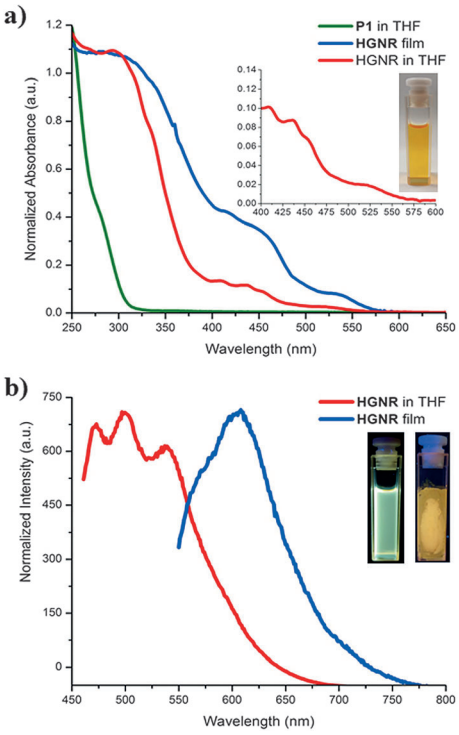

Figure 4. a) UV/Vis absorption spectrum of P1 (green line), HGNR in THF (red line), and HGNR in thin film (blue line). Inset: magnification of the 400 to 600 nm region of the spectrum in solution and a photo of a dilute solution of HGNR in $CHCl_3$ under ambient light. b) Photoluminescence spectrum of HGNR in THF (red line, λ_{ex} = 460 nm) and HGNR in thin film (blue line, λ_{ex} = 460 nm). Inset: dilute solution (left) and drop-cast film (right) of HGNR in $CHCl_3$ under UV (365 nm) light.

© 2017 Wiley-VCH Verlag GmbH & Co. KGaA, Weinheim

similar conformation in both solution and solid state, which is expected for a rigid π-conjugated backbone. Interestingly, a shoulder at 535 nm appeared in both the solution and solid-state spectra, which can be attributed to intramolecular π-stacking of the helical structure.[22] The optical band gap of HGNR measured at the absorption band onset is 2.15 eV, which is one of the highest measured to date for a GNR.

Fluorescence spectroscopy experiments were also performed in both solution and the solid state (Figure 4b). In solution, HGNR exhibits three vibronic emission bands located at 473, 500 and 538 nm. In thin film, the emission band is red-shifted by 69 nm at 607 nm, with a shoulder in the higher energy region (569 nm), close to the emission measured in solution. Although it is difficult in our case to gather direct experimental evidence of it, we hypothesize that this behavior can be attributed to an intramolecular excimer-like emission, as it is very similar to what has been observed in the case of foldamers based on conjugated units.[22,23]

Transmission electron microscopy (TEM) was performed to study the morphological features and structural parameters of HGNR. The results are shown in Figure 5. When a dispersion of HGNR (hexanes/CH_2Cl_2) was deposited on a copper grid, large aggregates of few microns were observed (Figures S24). As shown on Figure 5a, individual 1D, rigid nanostructures of identical diameter (55 Å) can be observed, which is in full agreement with the theoretical diameter of HGNR (54.9 Å). Interestingly, a slight change in the solvent mixture used for the preparation of the dispersion (hexanes/$CHCl_3$) induced a significant change in the morphology of the aggregates (Figure 5b). In fact, individual HGNR can no longer be seen, but well-organized arrays of 1D nanostructures can be observed and the width of these features (54.0 Å) agrees with the theoretical value of HGNR.

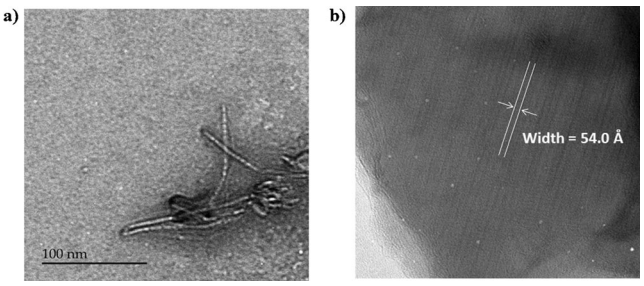

Figure 5. a) TEM image of HGNRs prepared from suspensions in hexanes/CH_2Cl_2. b) TEM image of HGNRs prepared from suspensions in hexanes/$CHCl_3$. Average measured width of HGNR = 54 Å.

In conclusion, we have prepared the first helical graphene nanoribbons (HGNR) from a polychlorinated poly(*m*-phenylene) precursor using the regioselective cyclodehydrochlorination (CDHC) reaction. ^{1}H NMR, FT-IR, XPS, TEM, and Raman spectroscopy confirmed that a GNR was formed during the process. HGNR has a rather large band gap compared to other GNRs reported to date and is highly emissive, both in solution and the solid state. The possibility of preparing such well-defined helical GNR structure opens up new opportunities for applications in host–guest chemistry, molecular electronics and sensing.

Acknowledgements

This research was supported by the NSERC through a Discovery Grant. M.D. thanks the FRQ-NT for a PhD scholarship. We would like to thank Pascale Chevallier (XPS) and Rodica Plesu (SEC) for their help in polymer characterization.

Conflict of interest

The authors declare no conflict of interest.

Keywords: carbon materials · graphene nanoribbons · helical polymer · helicenes · photochemistry

[1] a) K. S. Novoselov, A. K. Geim, S. V. Morozov, D. Jiang, Y. Zhang, S. V. Bubonos, I. V. Grigorieva, A. A. Firsov, *Science* **2004**, *306*, 666; b) K. S. Novoselov, A. K. Geim, S. V. Morozov, D. Jiang, M. I. Katsnelson, I. V. Grigorieva, S. V. Dubonos, A. A. Firsov, *Nature* **2005**, *438*, 197; c) D. R. Dreyer, R. S. Ruoff, C. W. Bielawski, *Angew. Chem. Int. Ed.* **2010**, *49*, 9336; *Angew. Chem.* **2010**, *122*, 9524; d) D. K. James, J. M. Tour, *Acc. Chem. Res.* **2013**, *46*, 2307.

[2] a) K. S. Novoselov, V. I. Fal'ko, L. Colombo, P. R. Gellert, M. G. Schwab, K. Kim, *Nature* **2012**, *490*, 192; b) G. Lu, K. Yu, Z. Wen, J. Chen, *Nanoscale* **2013**, *5*, 1353.

[3] a) K.-J. Jeon, Z. Lee, E. Pollak, L. Moreschini, A. Bostwick, C.-M. Park, R. Mendelsberg, V. Radmilovic, R. Kostecki, T. J. Richardson, E. Rotenberg, *ACS Nano* **2011**, *5*, 1042; b) H. Feng, R. Cheng, X. Zhao, X. Duan, J. Li, *Nat. Commun.* **2013**, *4*, 1; c) J. S. Oh, K. N. Kim, G. Y. Yeom, *J. Nanosci. Nanotechnol.* **2014**, *14*, 1120.

[4] X. Li, X. Wang, L. Zhang, S. Lee, H. Dai, *Science* **2008**, *319*, 1229.

[5] K. Müllen, *ACS Nano* **2014**, *8*, 6531.

[6] For a recent Review on GNRs synthesis, see: A. Narita, X.-Y. Wang, X. Feng, K. Müllen, *Chem. Soc. Rev.* **2015**, *44*, 6616.

[7] a) T. H. Vo, M. Shekhirev, D. A. Kunkel, M. D. Morton, E. Berglund, L. Kong, P. M. Wilson, P. A. Dowben, A. Enders, A. Sinitskii, *Nat. Commun.* **2014**, *5*, 1; b) J. Liu, B.-W. Li, Y.-Z. Tan, A. Giannakopoulos, C. Sanchez-Sanchez, D. Beljonne, P. Ruffieux, R. Fasel, X. Feng, K. Müllen, *J. Am. Chem. Soc.* **2015**, *137*, 6097.

[8] a) K. Ozaki, K. Kawasumi, M. Shibata, H. Ito, K. Itami, *Nat. Commun.* **2015**, *6*, 6251; b) B. T. King, J. KroulÌk, C. R. Robertson, P. Rempala, C. L. Hilton, J. D. Korinek, L. M. Gortari, *J. Org. Chem.* **2007**, *72*, 2279.

[9] P. Rempala, J. Kroulik, B. T. King, *J. Org. Chem.* **2006**, *71*, 5067.

[10] M. Daigle, A. Picard-Lafond, E. Soligo, J.-F. Morin, *Angew. Chem. Int. Ed.* **2016**, *55*, 2042; *Angew. Chem.* **2016**, *128*, 2082.

[11] F. Xu, H. Yu, A. Sadrzadeh, B. I. Yakobson, *Nano Lett.* **2016**, *16*, 34.

[12] M. M. Murray, P. Kaszynski, D. A. Kaisaki, W. Chang, D. A. Dougherty, *J. Am. Chem. Soc.* **1994**, *116*, 8152.

[13] K. Tahara, S. Okuhata, J. Adisoejoso, S. Lei, T. Fujita, S. D. Feyter, Y. Tobe, *J. Am. Chem. Soc.* **2009**, *131*, 17583.

[14] The use of di-*tert*-butylphosphine ferrocene (D*t*BPF) as the ligand was crucial to avoid competitive dehalogenation reaction. See: M. Murata, T. Sambommatsu, S. Watanabe, Y. Masuda, *Synlett* **2006**, 1867.

[15] B. Hohl, L. Bertschi, X. Zhang, A. D. Schlüter, J. Sakamoto, *Macromolecules* **2012**, *45*, 5418.

 © 2017 Wiley-VCH Verlag GmbH & Co. KGaA, Weinheim

These are not the final page numbers!

[16] S. Hecht, A. Khan, *Angew. Chem. Int. Ed.* **2003**, *42*, 6021; *Angew. Chem.* **2003**, *115*, 6203.
[17] D. Peña, A. Cobas, D. Pérez, E. Guitian, L. Castedo, *Org. Lett.* **2000**, *2*, 1629.
[18] A. Pradhan, P. Dechambenoit, H. Bock, F. Durola, *Angew. Chem. Int. Ed.* **2011**, *50*, 12582; *Angew. Chem.* **2011**, *123*, 12790.
[19] A. Centrone, L. Brambilla, T. Renouard, L. Gherghel, C. Mathis, K. Müllen, G. Zerbi, *Carbon* **2005**, *43*, 1593.
[20] a) W. Yang, A. Lucotti, M. Tommasini, W. A. Chalifoux, *J. Am. Chem. Soc.* **2016**, *138*, 9137; b) I. A. Verzhbitskiy, M. De Corato, A. Ruini, E. Molinari, A. Narita, Y. Hu, M. G. Schwab, M. Bruna, D. Yoon, S. Milana, X. Feng, K. Müllen, A. C. Ferrari, C. Casiraghi, D. Prezzi, *Nano Lett.* **2016**, *16*, 3442; c) U. Beser, M. Kastler, A. Maghsoumi, M. Wagner, C. Castiglioni, M. Tommasini, A. Narita, X. Feng, K. Müllen, *J. Am. Chem. Soc.* **2016**, *138*, 4322; d) A. Maghsoumi, L. Brambilla, C. Castiglioni, K. Müllen, M. Tommasini, *J. Raman Spectrosc.* **2015**, *46*, 757; e) M. Tommasini, G. Longhi, G. Mazzeo, S. Abbate, B. Nieto-Ortega, F. J. Ramírez, J. Casado, J. T. López Navarrete, *J. Chem. Theory Comput.* **2014**, *10*, 5520; f) C. Johannessen, E. W. Blanch, C. Villani, S. Abbate, G. Longhi, N. R. Agarwal, M. Tommasini, D. A. Lightner, *J. Phys. Chem. B* **2013**, *117*, 2221; g) J. Cai, P. Ruffieux, R. Jaafar, M. Bieri, T. Braun, S. Blankenburg, M. Muoth, A. P. Seitsonen, M. Saleh, X. Feng, K. Müllen, R. Fasel, *Nature* **2010**, *466*, 470; h) M. G. Schwab, A. Narita, S. Osella, Y. Hu, A. Maghsoumi, A. Mavrinsky, W. Pisula, C. Castiglioni, M. Tommasini, D. Beljonne, X. Feng, K. Mullen, *Chem. Asian J.* **2015**, *10*, 2134.
[21] C. Castiglioni, M. Tommasini, G. Zerbi, *Philos. Trans. R. Soc. London Ser. A* **2004**, *362*, 2425.
[22] K. Suda, K. Akagi, *Macromolecules* **2011**, *44*, 9473.
[23] a) R. B. Prince, J. G. Saven, P. G. Wolynes, J. S. Moore, *J. Am. Chem. Soc.* **1999**, *121*, 3114; b) W. Y. Yang, R. B. Prince, J. Sabelko, J. S. Moore, M. Gruebele, *J. Am. Chem. Soc.* **2000**, *122*, 3248.

Manuscript received: December 5, 2016
Final Article published: ■■ ■■, ■■■■

 © 2017 Wiley-VCH Verlag GmbH & Co. KGaA, Weinheim

Communications

Graphene Nanoribbons

M. Daigle, D. Miao, A. Lucotti, M. Tommasini, J.-F. Morin* _____ ▮▮▮▮–▮▮▮▮

Helically Coiled Graphene Nanoribbons

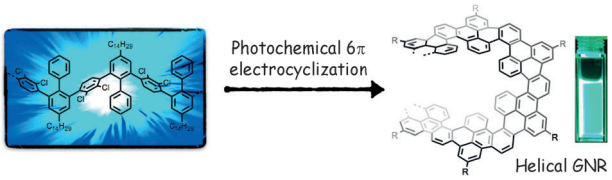

Made into ribbons: Helicene-like graphene nanoribbons (HGNR) have been prepared through a regioselective photochemical cyclodehydrochlorination (CDHC) reaction from a polychlorinated polyphenylene precursor.

© 2017 Wiley-VCH Verlag GmbH & Co. KGaA, Weinheim

These are not the final page numbers!